Observations of isoprene, methacrolein (MAC) and methyl vinyl ketone (MVK) at a mountain site in Hong Kong

H. Guo,[1] Z. H. Ling,[1] I. J. Simpson,[2] D. R. Blake,[2] and D. W. Wang[1]

Received 7 March 2012; revised 21 August 2012; accepted 25 August 2012; published 3 October 2012.

[1] A field campaign was carried out in September–November 2010 near the summit of Mt. Tai Mo Shan in Hong Kong. Isoprene, methyl vinyl ketone (MVK) and methacrolein (MAC) were measured. The average isoprene mixing ratio was 109 pptv, and the average MAC and MVK levels were 68 pptv and 164 pptv, respectively. The average daytime levels of isoprene (149 ± 20 pptv, average ± 95% confidence interval, $p < 0.01$), MAC (70 ± 9 pptv, $p < 0.01$) and MVK (169 ± 22 pptv, $p < 0.1$) were significantly higher than the average nighttime values (20 ± 5 pptv, 49 ± 8 pptv and 139 ± 25 pptv, respectively). The relationship between MVK and MAC indicated that nearby isoprene oxidation dominated their daytime abundances, while NO_3 chemistry and regional transport of anthropogenic sources from inland Pearl River Delta region could explain the higher MVK to MAC ratios at night. Correlation analysis of [MVK]/[isoprene] versus [MAC]/[isoprene] found that the isoprene photochemical ages were between 10 and 64 min. Regression analysis of total O_3 (O_3 + NO_2) versus MVK resulted in an estimated contribution of isoprene oxidation to ozone production of 12.5%, consistent with the simulated contribution of 10-11% by an observation-based model.

Citation: Guo, H., Z. H. Ling, I. J. Simpson, D. R. Blake, and D. W. Wang (2012), Observations of isoprene, methacrolein (MAC) and methyl vinyl ketone (MVK) at a mountain site in Hong Kong, *J. Geophys. Res.*, *117*, D19303, doi:10.1029/2012JD017750.

1. Introduction

[2] Volatile organic compounds (VOCs) are emitted in substantial quantities from both biogenic and anthropogenic sources [*Guenther et al.*, 1995; *Olivier et al.*, 1996]. These emissions have a major influence on the chemistry of the lower atmosphere, the oxidizing capacity of the atmosphere, visibility degradation, and consequently on the global climate [*Lacis et al.*, 1990; *Crutzen*, 1995; *Saunders et al.*, 2003]. It is estimated that about 80% of the global annual emissions of VOCs are associated with emissions from vegetation [*Warneck*, 2000]. Furthermore, the reactivity of biogenic VOCs (BVOCs) is estimated to be two to three times that of anthropogenic VOCs (AVOCs) [*Carter and Atkinson*, 1996; *Carter*, 1996; *Atkinson*, 1997]. Thus, even at lower concentrations than AVOCs, BVOCs can have a significant impact on air quality. BVOCs contribute to tropospheric ozone (O_3) and secondary particle formation via photo-oxidation in the presence of nitrogen oxides (NO_x) and sunlight [*National Research Council*, 1991]. The impact of BVOCs on O_3 and secondary particle formation becomes more prominent in hot seasons, when both photochemical activity and BVOC emissions are at a maximum. Therefore, photochemical oxidation of BVOCs has important implications for local and regional air quality, the greenhouse effect including ozone formation, acid production, and global climate change [*Intergovernmental Panel on Climate Change*, 1992].

[3] Isoprene, of biogenic origin, is of particular interest because it appears to have the largest significance among the BVOCs for boundary layer O_3 formation [*Carter and Atkinson*, 1996; *Carter*, 1996; *Atkinson*, 1997; *Guenther*, 2008]. In the atmosphere isoprene reacts mainly with O_3, OH and NO_3 radicals, with the subsequent production/regeneration of O_3 and photochemical oxidants. The major intermediate products generated from isoprene oxidation are methyl vinyl ketone (MVK) and methacrolein (MAC). Table 1 shows the key rate constants for isoprene, MVK and MAC. Although measurements of isoprene provide useful information regarding the potential for isoprene to contribute to O_3 production, concentration-time profiles of its oxidation products MVK and MAC provide a more direct measure of the actual rate of oxidation of isoprene, and subsequently its contribution to O_3 production [*Biesenthal et al.*, 1997]. Hence, in order to better understand the role that isoprene plays in the atmosphere, it is important to explore the relationship among isoprene and its photochemical products.

[4] A number of chamber studies have been carried out to examine the isoprene oxidation cycle [*Myoshi et al.*, 1994;

[1]Air Quality Studies, Department of Civil and Environmental Engineering, Hong Kong Polytechnic University, Kowloon, Hong Kong.
[2]Department of Chemistry, University of California, Irvine, California, USA.

Corresponding author: H. Guo, Air Quality Studies, Department of Civil and Environmental Engineering, Hong Kong Polytechnic University, Kowloon, Hong Kong. (ceguohai@polyu.edu.hk)

0148-0227/12/2012JD017750

Table 1. Rate Constants for Isoprene, MVK and MAC[a]

Compound	k_{O3}[b]	k_{OH}[b]	k_{NO3}	k_{Cl}[c]
Isoprene	1.28E-17	1.10E-10	6.16E-12[b]	4.0E-10
MVK	4.56E-18	1.88E-11	<6.00E-16[d]	2.2E-10
MAC	1.14E-18	3.35E-11	3.30E-15[d]	2.4E-10

[a]Unit: cm^3 $molecules^{-1}$ sec^{-1}.
[b]*Carter and Atkinson* [1996].
[c]*Apel et al.* [2002].
[d]*Kwok et al.* [1996].

Carter and Atkinson, 1996; *Iannone et al.*, 2009; *Navarro et al.*, 2011]. However, during daytime the evolution of isoprene chemistry in the real atmosphere is conceptually different from chamber experiments in that there is a continuous supply of isoprene [*Karl et al.*, 2009]. As such, field studies are essential to understanding isoprene chemistry. Indeed, many field studies have been conducted during the past two decades to study isoprene photochemistry in the world [*Yokouchi*, 1994; *Biesenthal et al.*, 1997; *Biesenthal and Shepson*, 1997; *Starn et al.*, 1998a; *Apel et al.*, 2002; *Dreyfus et al.*, 2002; *Spaulding et al.*, 2003; *Roberts et al.*, 2006; *Karl et al.*, 2009; *Jones et al.*, 2011; *Park et al.*, 2011]. These studies provide useful information about the isoprene oxidation mechanisms, and in particular, help to determine the conditions under which it is useful to control VOCs (e.g. VOC-limited environments) and the conditions under which this will have little effect [*Apel et al.*, 2002]. However, this kind of information is lacking in subtropical Hong Kong where the air quality is significantly affected by local emissions and regional transport [*Guo et al.*, 2009; *Jiang et al.*, 2010].

[5] Therefore a field measurement study of main air pollutants such as NO_x, O_3, $PM_{2.5}$, particle number concentrations, VOCs, carbonyl compounds, and meteorological data was carried out between 6 September and 29 November, 2010, near the summit and at the foot of Mt. Tai Mo Shan in Hong Kong. As a part of the project, a variety of anthropogenic and biogenic VOCs including isoprene, MVK and MAC were measured on 20 specifically selected days at the sites during the 3-month period. In this study, our focus was measurements from the summit of the mountain. The temporal variations of isoprene and its photochemical products were investigated; the relationship between isoprene and its photochemical products were explored, as was the relationship between the photochemical products; and the contribution of isoprene to the O_3 production was evaluated. Therefore the overall objective of this work is to better understand the isoprene oxidation mechanism in subtropical Hong Kong.

2. Experimental Setup

2.1. Site Description

[6] Mt. Tai Mo Shan (TMS) is the highest mountain in Hong Kong ((elevation = 957 m, see Figure 1). Enveloping this massif is 1440 hectares of natural territory (AFCD, http://www.afcd.gov.hk). There are forest plantations in the southeastern part of the mountain. The forest is mainly composed of *Acacia confusa*, *Lophotemon confertus*, *Machilus chekiangensis* and *Schima superba*, which are weak isoprene emitters [*Baker et al.*, 2005; *Leung et al.*, 2010]. Limited by climatic and geographic factors, these plantations end at the 550 m contour, above which shrubs and grasses dominate (AFCD, http://www.afcd.gov.hk). Surrounding the foot of the mountain are urban centers with a population of 2.23 million. The straight distances between the mountain summit and the urban centers at the foot are about 5–10 km. Farther to the south are the urban centers of the partial New Territory, Kowloon peninsula and Hong Kong Island. To the southwest is the newly-developed residential area of Tung Chung, the international airport and the South China Sea. To the west are the Tuen Mun residential areas and to the south is the South China Sea. To the north and northeast are the city clusters of the inland Pearl River Delta (PRD) region. The distance to the nearest city i.e. Shenzhen is only 15 km. Due to prevailing north/northeast synoptic winds in September–November, polluted air from inland PRD often reaches the sampling site. In addition, because of its unique topography, mountain-valley breezes and sea-land breezes are frequently observed at TMS. These mesoscale circulations enhance the interaction of polluted urban air and the mountain air. The sampling site was set on the rooftop of a building at the waist of TMS (22.405°N, 114.118°E; 640 m a.s.l.).

2.2. Measurement Techniques

2.2.1. Continuous Measurements of O_3, CO and NO-NO_2-NO_x

[7] At TMS, measurement instruments were installed inside a 3-storey building. Ambient air samples were drawn

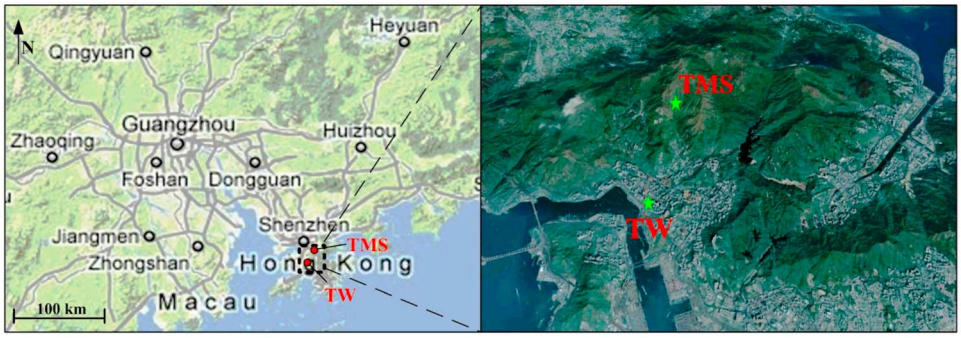

Figure 1. Location of the sampling sites, Hong Kong. Tai Mo Shan (TMS) site is near the summit of the mountain and Tsuen Wan (TW) site is at the foot of the mountain.

through a 5 m long perfluoroalkoxy (PFA) Teflon tube (OD: 12.7 mm; ID: 9.6 mm). The sampling tube inlet was located 2 m above the rooftop of the building. The other end of the sampling tube was connected to a PFA manifold with a bypass pump drawing air at a rate of 5 L min^{-1}. The intake of the O_3, CO and NO-NO_2-NO_x analyzers was connected to the manifold.

[8] Ozone was measured using a commercial UV photometric instrument (Advanced Pollution Instrumentation (API), model 400E) that has a detection limit of 0.6 ppbv. The analyzer was calibrated by a transfer standard (TEI 49PS) prior to the field studies. Sulfur dioxide was measured by a pulsed UV fluorescence (API, model 100E) with a detection limit of 0.4 ppbv and 2-σ precision of 0.5% for ambient levels of 50 ppbv (2-min average). To address the challenges of background and low level CO monitoring, a gas filter correlation trace level CO analyzer was used (API, Model 300EU). Using a gas filter correlation wheel, a high energy infrared source alternatively passes through a CO filled chamber and a chamber with no CO present. The light path then travels through the sample cell. The energy loss through the sample cell is compared with the zero reference provided by the gas filter to produce a signal proportional to concentration. Oxides of nitrogen were measured with an API-Teledyne Model 200e analyzer, utilizing chemiluminescence and configured by the manufacturer to report data with 20-s time resolution. The analyzer has a detection limit of 0.4 ppbv. The Model 200E is a single chamber, single photomultiplier tube design which cycles between the NO, NO_x, and zero modes. The addition of the zero mode provides excellent long term stability and low minimum detectable limits. However, the NO_x measurement by chemiluminescent method has potential interference from nitric acid, PAN and other atmospheric nitrates.

[9] The analyzers were calibrated daily by injecting scrubbed ambient air (TEI, Model 111) and a span gas mixture. A NIST-traceable standard (Scott-Marrin, Inc.) containing 156.5 ppmv carbon monoxide (CO) ($\pm$2%), 15.64 ppmv SO_2 ($\pm$2%), and 15.55 ppmv NO ($\pm$2%) was diluted using a dynamic calibrator (Environics, Inc., Model 6100). A data logger (Environmental Systems Corporation, Model 8832) was used to control the calibrations and to collect data, which were averaged to 1-min values.

[10] In addition to the above chemical measurements, several meteorological parameters including temperature, solar radiation, wind speed and wind direction were monitored by an integrated sensor suite (Vantage Pro TM & Vantage Pro 2 Plus TM Weather Stations, Davis Instruments).

2.2.2. Sampling and Analysis of VOCs

[11] VOC samples were collected on selected non-O_3 episode (i.e. 28 Sept., 02, 08, 14, 18–19, 27–28 Oct., 20–21 Nov., 2010) and O_3 episode days (e.g. 23–24 Oct., 29 Oct. 03 Nov., 09 Nov. and 19 Nov.). In this study, an O_3 episode day was defined as a day when the actual highest hourly O_3 concentration exceeded 200 $\mu g/m^3$ ($\sim$102 ppbv) based on the Ambient Air Quality Standard in China (China's Grade II standard, http://english.mep.gov.cn/standards_reports/standards/Air_Environment/quality_standard1/200710/t20071024_111819.htm) in terms of the regional context. The potentially high O_3 episode days were selected on the basis of weather prediction and meteorological data analysis, which were usually related to stronger solar radiation, weaker wind speed, and less vertical dilution of air pollution compared to the non-O_3 episode days. Ambient VOC samples were collected using cleaned and evacuated 2-L electro-polished stainless steel canisters. The canisters were prepared and delivered to Hong Kong by the Rowland/Blake group at University of California, Irvine (UCI). A stainless steel flow-controlling device was used to collect 1-h integrated samples i.e. filled up the vacuum canister to 40 psi in one hour. During non-O_3 episode days, hourly VOC samples were collected from 7 a.m. to 7 p.m. (one sample every two hours) per day. For O_3 episode days, hourly samples were consecutively collected from 9 a.m. to 4 p.m. with additional samples collected at 6 p.m., 9 p.m., 12 midnight, 3 a.m. and 7 a.m. per day. Totally, 201 VOC samples were collected at TMS.

[12] After sampling, the whole air samples were returned to the laboratory at UCI for chemical analysis. Although we reported only isoprene, MVK and MAC here, 73 VOC species were quantified in this project. It is noteworthy that international intercomparison experiments have demonstrated that the analytical procedures in the UCI's lab consistently yield accurate identification of a wide range of unknown hydrocarbons and produces excellent quantitative results [e.g., *Apel et al.*, 1999, 2003; *Karl et al.*, 2007]. One example is the Tropical Forest and Fire Emissions Experiment (TROFFEE) in the Amazon basin, in which isoprene samples collected in canisters during the research flights were compared with the online proton transfer reaction mass spectrometry (PTRMS) measurements [*Karl et al.*, 2007]. Excellent agreement between these two methods was shown (PTR-MS/GC-FID: 1.13, R^2 = 0.96), suggesting minimal interference due to the presence of other VOCs. The canister method was also compared with sorbent cartridges in *Kuhn et al.* [2007]. Reasonable agreement was achieved for isoprene mixing ratios derived by cartridges analyzed with GC-FID and canister samples (slope = 1.04, R^2 = 0.62).

[13] The analytical systems are described as follows [*Colman et al.*, 2001; *Simpson et al.*, 2010]. The whole system included multicolumn gas chromatography. The first HP-6890 (GC-1) contained two columns. The first column was a J&W DB-5 (30 m; i.d., 0.25 mm; film ,1 μm) connected in series to a RESTEK 1701 (5 m; i.d., 0.25 mm; film, 0.5 μm), which was output to an ECD detector. The DB-5/RESTEK 1701 union helped to resolve halocarbon and organic nitrate species that have similar polarity through higher retention of the nitrate species. The second column was a DB-5 ms (60 m; i.d., 0.25 mm; film, 0.5 μm), which was output to an MSD detector (HP-5973). The DB-5/RESTEK 1701 received 6.84% of the total carrier flow, and the DB-5 ms received 10.10%. The second HP-6890 (GC-2) contained a J&W DB-1 column (60 m; i.d., 0.32 mm; film, 1 μm) output to an FID detector. This column received 15.10% of the flow. The third HP-6890 (GC-3) contained a J&W GS-Alumina PLOT column (30 m,; i.d., 0.53 mm) connected in series to a DB-1 (5 m; i.d., 0.53 mm; film, 1 μm), which was output to a FID detector, and a RESTEK 1701 (60 m; i.d., 0.25 mm; film, 0.50 μm), which was output to an ECD detector. The PLOT/DB-1 union helped to reduce signal spikes from PLOT column bleed and tightened up the CO_2 peak width. The GS-Alumina PLOT column received

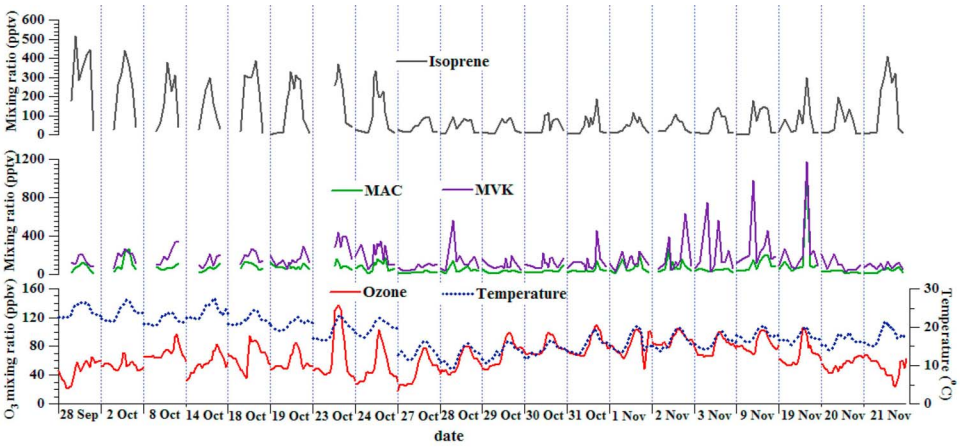

Figure 2. Time series of (top) isoprene, (middle) MAC and MVK and (bottom) ozone and temperature. The figure is drawn using hourly measurement data with the aid of Igor Plot software.

60.80% of the flow, and the RESTEK 1701 received the remaining 7.16%. The oven parameters employed for each GC can be found in *Colman et al.* [2001]. Liquid nitrogen was used to achieve subambient initial temperatures.

2.2.3. Quality Control and Assurance for VOCs

[14] Before sampling, all canisters were cleaned at least five times by repeatedly filling and evacuating them with humidified pure nitrogen gas. In order to check whether there was any contamination in the canister, we filled the evacuated canisters with pure N_2 and stored them in the laboratory for at least 24 hours. These canisters were then checked by the same VOC analytical method to ensure that all the target compounds were not found or were under the method detection limit. In addition, duplicate samples were regularly collected to check the precision and reliability of the sampling and analytical methods.

[15] The quantification of target VOCs was accomplished using multi-point external calibration curves, using a combination of National Bureau of Standards, Scott Specialty Gases (absolute accuracy estimated to be within ±5%) and UCI-made standards. Calibration was an ongoing process whereby new standards were referenced to older certified standards, with appropriate checks for stability and with regular interlaboratory comparisons. Multiple standards were used during sample analysis, including working standards (analyzed every four samples) and absolute standards (analyzed twice daily). The measurement precision, accuracy and detection limits of the VOCs varied by compound and were periodically quantified for each species during the sampling period. Detailed procedures are described in *Simpson et al.* [2010, 2011]. Briefly, the measurement precision for the alkanes, alkenes (including isoprene) and alkynes is 3%, 5% for aromatics, and 30% for MVK and MAC. The measurement accuracy for alkanes, alkenes, alkynes and aromatics is 5%, and 20% for MVK and MAC. The limit of detection is 3 pptv for the non-methane hydrocarbons (NMHCs) including isoprene, and 5 pptv for MVK and MAC. It is worth noting that a strong correlation between MVK and MAC (R^2 = 0.87) in our previous study [*Simpson et al.*, 2010] enhanced our confidence in the data quality in this study, as both studies used the same analytical and quality control procedures and the concentration ranges of MVK and MAC were similar.

3. Results and Discussion

3.1. Temporal Variations of Isoprene, MVK and MAC

3.1.1. Day-to-Day Variations

[16] Figure 2 shows time series plots for isoprene, MVK and MAC measurements obtained during the study. In addition, time series of O_3 and temperature are also given. Large day-to-day variations were observed for isoprene, MAC and MVK. The average isoprene level during the entire sampling period was 109 pptv (2–517 pptv), and the average MAC and MVK mixing ratios were 68 pptv with a range of 8–1056 pptv and 164 pptv ranging from 27–1171 pptv, respectively. There was a clear decrease in both isoprene abundance and ambient temperature starting on 27 October ($p < 0.001$). Interestingly, this cooler period (i.e. 27 October–20 November) had more O_3-episode days, which was discussed in detail in H. Guo et al. (Characterization of photochemical pollution at different elevations in mountainous areas in southern China, submitted to *Atmospheric Chemistry and Physics*, 2012). In particular, from 2 to 19 November, MVK values increased substantially, probably caused by anthropogenic sources since MAC and isoprene were seemingly unaffected, and higher MVK mixing ratios than isoprene were often observed. More detailed discussion on the potential anthropogenic sources is given in Section 3.1.3. Indeed, the average isoprene mixing ratio on non-O_3 episode days (150 ± 29 pptv) (average ± 95% confidence interval) was much higher than that on O_3 episode days (78 ± 15 pptv, $p < 0.01$), whereas the average MVK value on non-O_3 episode days (136 ± 17 pptv) was lower than that on O_3 episode days (186 ± 32 pptv, $p < 0.01$), indicating that isoprene might be destroyed more rapidly and more MVK was produced on O_3 episode days when photochemical reactions were stronger, and/or that isoprene emissions were lower and transport of MVK from anthropogenic sources to the mountain site increased MVK levels on O_3 episode days. The latter was likely true as the temperature was substantially lower on the majority of the

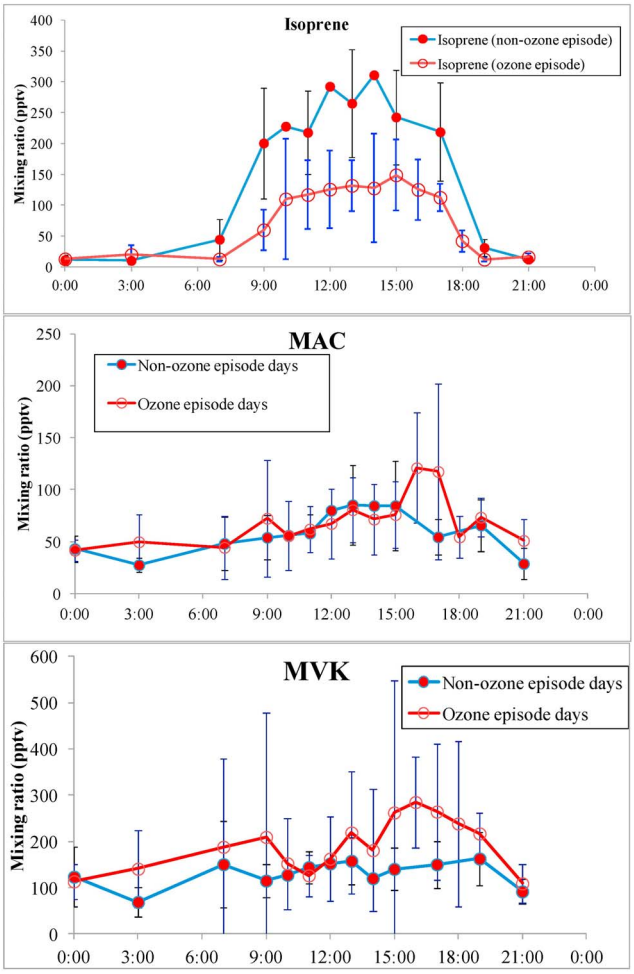

Figure 3. Average diurnal patterns of (top) isoprene, (middle) MAC and (bottom) MVK during the study. Error bars represent the spread in measurements in terms of 95 percent confidence interval.

O_3 episode days (16.6 ± 0.3 °C vs. 19.7 ± 0.6°C; $p < 0.001$), which would have a significant impact on the ambient levels of isoprene measured. The positive correlation between isoprene mixing ratio and temperature found in next section (i.e. Section 3.1.2) was evidence.

[17] The isoprene level in this study is similar to that (maximum concentration: 98 pptv) observed in summer above a boreal coniferous forest in Central Finland where low isoprene emitting trees were observed [*Hakola et al.*, 2003], the level (average: 146 ± 38 pptv) found in autumn 2002 in rural Hong Kong [*Wang et al.*, 2005], and the values (40–280 pptv) measured in spring at rural sites in the inland PRD region [*Tang et al.*, 2007]. However, the isoprene mixing ratio in this study is lower than that observed in autumn at an urban site in Hong Kong (average: 271 ± 52 pptv) [*Guo et al.*, 2009], in summer at rural and urban sites in Hong Kong (1028 ± 25 pptv and 1333 ± 21 pptv, respectively) [*Chen et al.*, 2010], and in 2000–2001 at three sites in Hong Kong (300, 430 and 460 pptv, respectively) [*So and Wang*, 2004]. It is also lower than the summer observations (maximum value: 5.3 ppbv) in the Lower Fraser Valley, Canada, which contained substantial vegetation in the form of deciduous and coniferous trees as well as agricultural crops [*Biesenthal et al.*, 1997], at a rural forested site (daytime median: 1.96 ± 0.26 ppbv) in Michigan where the dominant isoprene source was *Populous tremuloides* [*Apel et al.*, 2002], and in a South-East Asian tropical rainforest (daytime average: ~1ppbv) [*Jones et al.*, 2011]. The different isoprene levels among the different locations in different seasons and years are related to the vegetation types, temperature, light flux, and other meteorological parameters. More detailed discussion on the low isoprene levels found at the study site is given in section 3.1.2.

[18] The average MAC and MVK mixing ratios in this study are consistent with those reported by *Apel et al.* [2002] (daytime median: 60 ± 20 pptv and 100 ± 20 pptv, respectively) and *Hakola et al.* [2003] (10–180 pptv and 10–460 pptv, respectively), and are lower than those found by *Biesenthal et al.* [1997] (maximum value: 1000 pptv and 2000 pptv, respectively). *Apel et al.* [2002] found that the MAC and MVK levels in temperate Michigan were determined by the isoprene oxidation, whereas both isoprene oxidation and vehicular emissions affected the MAC and MVK levels at a boreal coniferous forest [*Hakola et al.*, 2003] and in the Lower Fraser Valley in Canada [*Biesenthal et al.*, 1997].

3.1.2. Diurnal Variations

[19] The diurnal behaviors of VOCs are affected by a number of chemical and meteorological factors. Figure 3 shows the average diurnal patterns of isoprene, MAC and MVK. It is evident that isoprene mixing ratios increased steadily commencing at 7 a.m., reaching a maximum level in early afternoon, and then gradually decreased to low levels at night, which remained until 7 a.m. of the next day. The higher isoprene mixing ratios in the daytime indicated that isoprene was being produced more rapidly than it was being destroyed from the time it was emitted to the time it was detected. The average daytime levels of isoprene (149 ± 20 pptv; two-tail *t*-test: $p < 0.01$), MAC (70 ± 9 pptv; two-tail *t*-test: $p < 0.01$) and MVK (169 ± 22 pptv; two-tail *t* test: $p < 0.1$) were significantly higher than the average values at night (20 ± 5 pptv, 49 ± 8 pptv and 139 ± 25 pptv, respectively). The causes for much lower nighttime isoprene mixing ratios have been well addressed in literature [e.g., *Cleveland and Yavitt*, 1997; *Hurst et al.*, 2001; *Apel et al.*, 2002; *Sillman et al.*, 2002]. The decreasing rate for MAC (30%) from daytime to nighttime was higher than that of MVK (18%), partly consistent with the fact that the reaction rate of MAC with nighttime NO_3 is faster than that of MVK with NO_3 (Table 1). Interestingly, the nighttime MVK and MAC levels remained high, similar to the results obtained by *Stroud et al.* [2001] who claimed that nighttime chemical oxidation and/or deposition of these products was slow at the urban forested site, but much higher than the values in rural canopy studies of *Montzka et al.* [1993], *Biesenthal et al.* [1997] and *Apel et al.* [2002]. However, *Karl et al.* [2010] found that MVK and MAC can be deposited to vegetation fairly efficiently, dependent on stomatal conductance and surface wetness. In this study, due to the complex topography surrounding the site, it suggested that a combination of isoprene photochemistry nearby, regional transport of anthropogenic sources, mesoscale circulation, and nighttime deposition and chemistry played an important role in

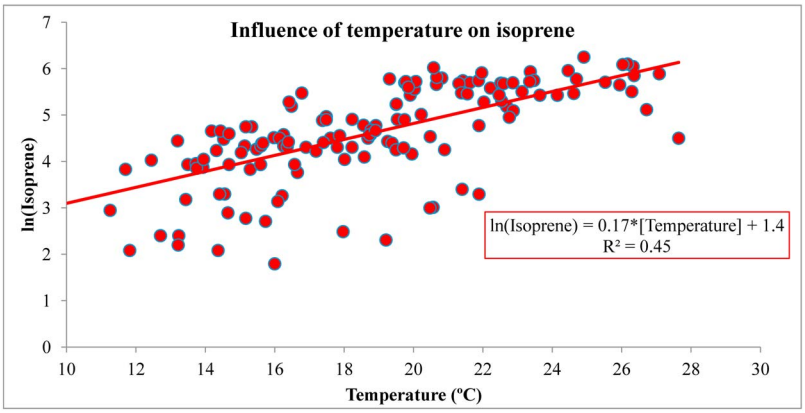

Figure 4. Scatterplots of isoprene versus temperature at daytime hours (07:00–18:00 local time) (139 data points. $p < 0.001$).

the diurnal patterns of MAC and MVK. More detailed discussion is given in section 3.1.3.

[20] It is well documented that the diurnal profile of isoprene is generally attributed to an emission pathway dependent upon both solar radiation and temperature [*Apel et al.*, 2002; *Kuhn et al.*, 2002; *Jones et al.*, 2011]. In this study, daytime isoprene was found to have some correlation with temperature (R^2 = 0.45) and a poor correlation with solar radiation (R^2 = 0.16, data not shown here) (Figure 4). The weak relationship between isoprene and temperature strongly indicated that isoprene chemistry dominated over isoprene emission rates as the driver of ambient abundances at the site. The poor correlation between isoprene and light suggests that there may be a time lag between when the isoprene was emitted (an upwind source) and when it was detected at the site. Moreover, changes in isoprene flux could vary rapidly with changes in light levels. Therefore quickly changing light conditions may not be reflected in the measured concentrations. However, temperature changes were considerably slower and more gradual and thus yielded a better correlation.

[21] To study isoprene oxidation and its importance in determining the observed levels of MAC and MVK, it is instructive to look at the diurnal trend in the MVK/MAC ratio [*Stroud et al.*, 2001]. Figure 5 presents the daytime and nighttime MVK versus MAC scatterplots during the study. Samples with potential anthropogenic sources of MVK were not included in Figure 5. Good correlations (R^2 = 0.59 and 0.67 for daytime and nighttime data, respectively) between MAC and MVK suggested their common source of isoprene oxidation at the site. As shown in the figure, the daytime ratio was 1.70 ± 0.12 (average ± standard error), consistent with the observations of many studies which showed a daytime ratio of ~2 [*Montzka et al.*, 1993; *Yokouchi*, 1994; *Biesenthal and Shepson*, 1997; *Stroud et al.*, 2001; *Apel et al.*, 2002; *Hakola et al.*, 2003; *Park et al.*, 2011]. However, this ratio had a slight increase (1.83 ± 0.17; two-tail *t* test: p = 0.04) at night at this mountain site, similar to the observations of *Biesenthal et al.* [1997], and much higher than that in other studies which found the nighttime ratio was about 1 [*Montzka et al.*, 1993; *Yokouchi*, 1994; *Stroud et al.*, 2001; *Apel et al.*, 2002; *Spaulding et al.*, 2003]. As measured in the lab by *Carter and Atkinson* [1996], the daytime oxidation of isoprene by OH yields an MVK/MAC ratio of ~1.4. The larger ratio observed in this study and previous studies than that predicted from lab studies was due to the fact that consumption of MAC via reaction with OH is faster than for MVK during daytime hours, and the reaction of isoprene with atomic chlorine (Cl) is considerably faster than the reactions of isoprene with OH and O_3 (Table 1), yielding ~14% MVK [*Fan and Zhang*, 2004]. Moreover, the higher daytime MVK/MAC ratios in this study could be also caused by the transport of MVK from anthropogenic sources in urban Hong Kong and/or neighbor cities in inland PRD to the sampling site, driven by mesoscale circulations and synoptic northerly winds, respectively. Indeed, chemical transport model simulation indicated the influence of mesoscale circulations and the predominance of synoptic northerly winds on the days when suspected anthropogenic MVK samples were observed (see Figure 2). Detailed discussion on the mesoscale circulations is given in Guo et al. (submitted manuscript, 2012).

[22] The nighttime ratio observed in this study was also higher than most other studies [*Montzka et al.*, 1993; *Yokouchi*, 1994; *Stroud et al.*, 2001; *Apel et al.*, 2002; *Spaulding et al.*, 2003]. NO_3 is a potentially important oxidant for nighttime chemical reactions. There was sufficient NO_2 and O_3 at night at this mountain site (Guo et al., submitted manuscript, 2012). The preferential reaction of NO_3 with MAC compared to MVK (Table 1) would result in an increase in the MVK/MAC ratio. It is noteworthy that due to the fact that sparse plantations exist above 550 m elevation, one would expect that isoprene-poor air transport from mountain summit (957 m elevation) downhill past the TMS site (640 m elevation) at night. Consequently, isoprene chemistry could not be significant during the nighttime hours. However, regional transport of MVK-laden air could also affect the nighttime MVK/MAC ratio at the site due to subsidence at the mountaintop, followed by downslope drainage. Detailed discussion is provided in section 3.1.3.

[23] According to the isoprene oxidation mechanism and previous field measurement results, the daytime and nighttime MVK/MAC ratios are ~2 and ~1, respectively, if only isoprene oxidation dominates [*Montzka et al.*, 1993; *Biesenthal et al.*, 1997; *Stroud et al.*, 2001; *Apel et al.*, 2002]. The daytime MVK/MAC ratio of 1.70 ± 0.12 in this study suggested the dominance of isoprene oxidation.

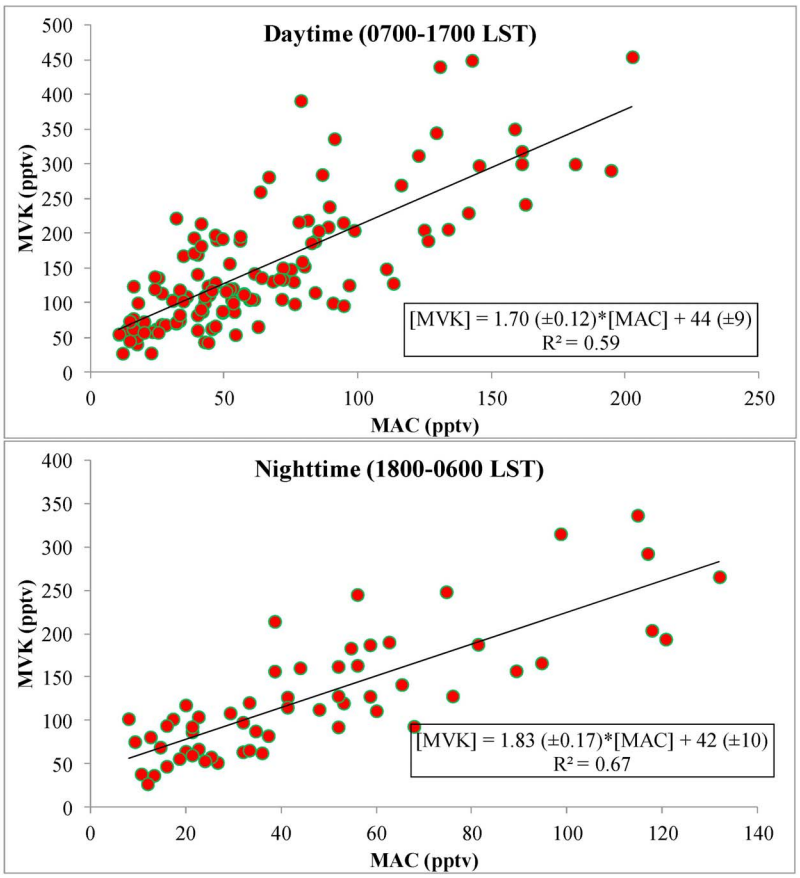

Figure 5. (top) Daytime and (bottom) nighttime correlations of MVK and MAC (data points: 129 and 59 for day and night, respectively. $p < 0.001$ for both correlations).

However, as stated above, there were a few (n = 9) daytime samples with very high MVK values, indicating the interference of anthropogenic MVK sources to the isoprene oxidation. In contrast, about twice (1.83 ± 0.17) the theoretical nighttime MVK/MAC ratio (~1) found in this study did give some indication that there must be some influence on MVK and MAC other than isoprene oxidation at night. Except for some outliers (n = 3) with extremely high MVK values which were most likely attributed to anthropogenic sources, the higher nighttime MVK/MAC ratio in this study than the theoretical ratio was probably related to the NO_3 chemistry and regional transport of MVK-laden air, as described above. Moreover, it could be also possible that the deposition rate of MAC was faster than that of MVK, leading to higher than expected MVK/MAC ratios at night. However, these deposition rates are not well known and one would not expect them to differ greatly.

3.1.3. Influence of NO_3 Chemistry, Mesoscale Circulations and Regional Transport on Nighttime MVK and MAC

[24] It is well documented that OH radical is mainly responsible for the daytime isoprene chemistry while NO_3 becomes more important to the oxidation of isoprene, MAC and MVK at night [*Carter and Atkinson*, 1996; *Starn et al.*, 1998b; *Vrekoussis et al.*, 2007; *Kim et al.*, 2011]. The NO_3 radicals are mainly formed via reaction $NO_2 + O_3 \rightarrow NO_3 + O_2$. In contrast, NO_3 radicals are removed by reactions in the gas phase with NO to form NO_2, and with NO_2 to form N_2O_5, in addition to the reactions with NMHCs [*Atkinson*, 2000]. At this mountain site, the average nighttime (18:00–06:00 LST) NO_2 (i.e. 6.1 ± 0.3 ppbv, average ± 95% confidence interval) and O_3 mixing ratios were high (i.e. 53 ± 1 ppbv), implying it was more favorable to the NO_3 formation. The nighttime NO_3 level at the site could be simply estimated by running a Master Chemical Mechanism (MCM) model using the measured nighttime O_3 and NO_x data. The simulation results showed the average nighttime NO_3 level was 11.3 ± 1.3 pptv, within the range found in the United States, and European continental and marine boundary layer [*Geyer et al.*, 2001; *Stroud et al.*, 2002; *Vrekoussis et al.*, 2004, 2007]. Hence, although the reaction rates of MAC and MVK with O_3 and NO_3 are low (Table 1), the nighttime chemical processing of these species could be significant due to high NO_3 levels at the site, leading to high nighttime MVK/MAC ratios. In addition, the diurnal behaviors of MAC and MVK showed an initial increase or stable values just as the boundary layer became stable (~18:00 local time) because there was still some residual photochemistry in the evening with low light levels and a small boundary layer volume (Figure 3). However, it ceased as night progressed and photochemistry was curtailed.

[25] Apart from the high nighttime MVK/MAC ratios potentially caused by the NO_3 chemistry and regional transport of MVK-laden air, high nighttime levels of MVK

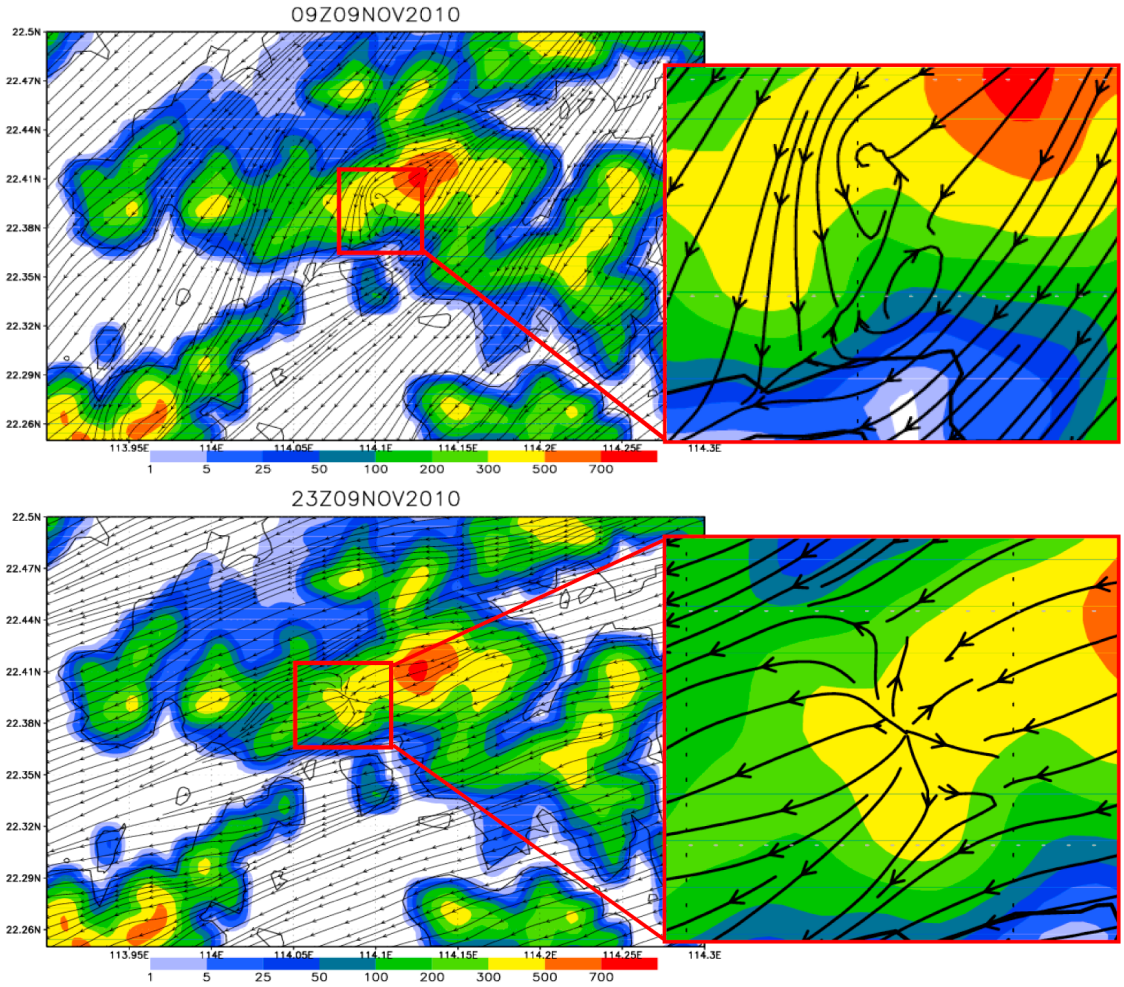

Figure 6. Simulation of mountain-valley breeze on 9 November 2010: (top) valley breeze in the daytime; (bottom) mountain breeze at nighttime.

and MAC were also found during the sampling period. To identify the potential sources of these high MVK and/or MAC samples, we first looked at the possible association of nighttime air at the site with mesoscale circulations i.e. mountain-valley flows using the Weather Research and Forecasting (WRF) model. As mountain-valley breezes are very small scale weather phenomenon caused by thermal forcing, and there is very complex terrain in Hong Kong, considerably high model resolution is needed in order to capture these breezes. In this study, the mountain-valley breezes were simulated using a domain system of five nested grids (36, 12, 4, 1.333, and 0.444 km). The domain with finest resolution (0.444 km grid) covers the Hong Kong region. The modeling focused on 16–18, 23 September, 23–24, 29–31 October, 1–3, 9, 12, and 19 November, 2010, when evidence for the mesoscale circulation was clear based on the meteorological data and the levels of air pollutants (Figure 6). Although the model results showed a valley breeze in the daytime (09:00, LST) and a mountain breeze at night (23:00, LST), the mesoscale flows were weak. The northerly synoptic winds dominated both daytime and nighttime flows near the mountain site (i.e. TMS). The features suggested that the daytime levels of MAC and MVK at the TMS site could be affected by the air at the foot of the mountain, while the nighttime MAC and MVK values at the sampling site were mainly influenced by the air from the summit followed by downslope drainage. However, as stated earlier, the plantations ended at the 550 m contour, lower than the height of the sampling site (640 m), suggesting isoprene-poor air arriving at the sampling site at night. Hence, the high nighttime MAC and MVK levels were more related to anthropogenic sources.

[26] Initial analyses of wind roses for the sampling period found that air masses reaching the site at both daytime and nighttime hours were mainly from the north directions i.e. polluted inland PRD region (Figure 7). To better understand the source origins of specific air masses, concentration ratios of SO_2 to NO_x were analyzed for all nighttime samples with high levels of MVK and MAC (denoted as values larger than their average values i.e. 139 pptv for MVK and 49 pptv for MAC, and MVK/MAC > 2.84; in total 19 cases), as they can provide signatures of air masses arriving at the site. The SO_2/NO_x ratio was found to be 0.38 ± 0.05 ppbv/ppbv. Previous studies indicated that the air masses from PRD are laden with relatively abundant SO_2 while the air masses in Hong Kong have high NO_x levels, and the SO_2/NO_x ratio for PRD air masses was 0.4–1.26 while it ranged from 0.12 to 0.29 for Hong Kong air masses [*Zhang et al.*, 1998; *Wang*

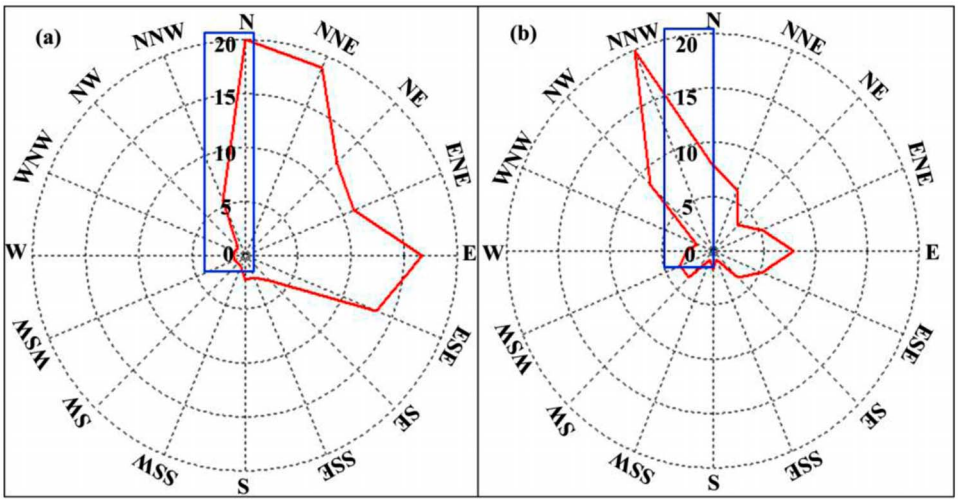

Figure 7. (a) Nighttime and (b) daytime wind roses during the sampling period.

et al., 2005; *Guo et al.*, 2009]. Hence, the nighttime samples with high levels of MVK and MAC were most likely originated from inland PRD region, further confirming the influence of anthropogenic MVK and MAC sources from the region.

[27] Anthropogenic MVK and MAC were reported to be emitted from motor vehicles and industrial sources [*Ingham et al.*, 1994; *Biesenthal and Shepson*, 1997; *New Jersey Department of Health and Senior Services* (*NJDHSS*), 2000, 2001; *Park et al.*, 2011]. As such, correlation analyses of MVK with the combustion tracer ethene, and MAC with its precursor *i*-butene for the MVK- and MAC-laden air masses were conducted, respectively. Some correlations between ethene and MVK (R^2 = 0.38, $p < 0.001$), and between *i*-butene and MAC (R^2 = 0.45, $p < 0.001$) suggested the possible contribution of vehicular combustion to MVK and MAC at the site from inland PRD. Tracers with similar lifetimes to MVK and MAC were selected for correlation analyses to avoid the influence of reactivity variations on the observed correlations. In addition, industrial sources can directly emit MVK and MAC to the atmosphere since MVK is used in synthesis of plastics, steroids and vitamin A, and the primary use of MAC is in the manufacture of polymers and synthetic resins [*NJDHSS*, 2000, 2001]. However, as other markers than MVK and MAC from pharmaceutical and chemical synthesis plants are unknown in the region, solid conclusion was unable to be drawn on the industrial sources in this study. Nevertheless, there are many petrochemical and pharmaceutical factories in the inland PRD region. Hence, the potential association between industrial sources in inland PRD and high level nighttime MAC and MVK at the site needs further investigation in the future.

3.2. Relationship Between Isoprene and Its Photochemical Products

[28] Since MVK and MAC are dominant first-generation reaction products from isoprene oxidation, a relationship is expected between mixing ratios of isoprene and these species as well as between the species themselves, if there are no other sources such as vehicular emissions (MVK/MAC ratio: ~2) and industrial sources [*Biesenthal and Shepson*, 1997; *NJDHSS*, 2000, 2001]. The scatterplots of daytime isoprene versus MVK and MAC (101 data points) are shown in Figure 8. Clearly, the correlations of isoprene with MAC (R^2 = 0.24, $p < 0.001$) and MVK (R^2 = 0.19, $p < 0.01$) were poor. To eliminate the possible influence of low isoprene

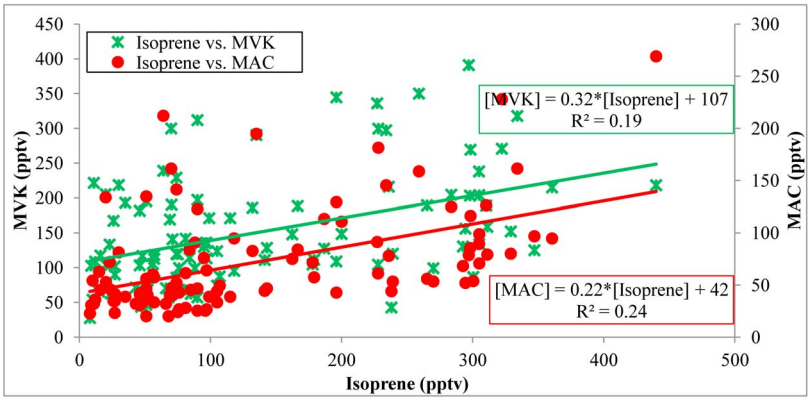

Figure 8. Scatterplots of daytime isoprene versus MAC and MVK (07:00–16:00; 101 data points. $p < 0.001$ and $p < 0.01$ for MAC and MVK, respectively).

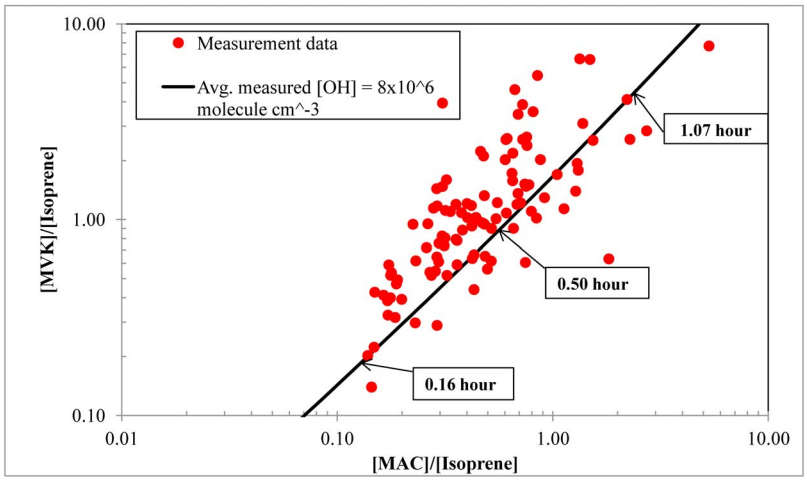

Figure 9. Plot of the measured MVK/isoprene versus MAC/isoprene ratios and the calculated ratio based on a consecutive reaction scheme model.

mixing ratios on the poor correlations, the lowest 10% of the isoprene data (i.e. 10 samples with the lowest isoprene levels) were removed and the correlations were re-analyzed. It was found the correlations were not improved (R^2 = 0.24 and 0.18 for MAC and MVK, respectively). Moreover, although we tried lagging the isoprene concentrations relative to the MAC and MVK, the correlations were also not improved (R^2 = 0.19 and 0.18, respectively). As isoprene levels are related to temperature and solar radiation, the correlations of its oxidation products i.e. ln(MAC) and ln(MVK) with temperature and light during daytime hours were also explored. Poor correlations (R^2 <0.26 and <0.07, respectively) were found. The lack of correlation between MVK and MAC with isoprene during daytime hours suggests that "local" isoprene was probably not responsible for most of the MVK and MAC. Since Figure 5 implied that isoprene oxidation was the primary source of MVK and MAC, it meant that upwind isoprene production was the primary source, i.e. isoprene that was emitted and mostly reacted away before reaching the sampling site. This was obvious as the emitting trees were further below on the mountain as described in the "sampling site" section. Moreover, the MVK/MAC ratio (1.70 ± 0.12) in this study was clearly indicative of a distant source but the lack of an even higher ratio also meant that the source was relatively nearby, or that the chemistry was relatively slow. Occasionally, anthropogenic emissions i.e. vehicular exhaust and/or industrial sources could lower the correlations between isoprene and its photochemical products. The poor correlations of isoprene with MAC and MVK found in this study are consistent with the observations of *Biesenthal et al.* [1997] and *Jones et al.* [2011] during studies in western Canada and south-east Asia, respectively.

[29] The ratios of MAC/isoprene and MVK/isoprene yield useful information on the transport time (photochemical age) of isoprene in an air mass [*Stroud et al.*, 2001; *Apel et al.*, 2002]. Since the sampling site was at the upper boundary of dense plants and trees, isoprene mixing ratios should be dominated by upwind emissions from the lower part of the mountain (which had much higher isoprene concentrations) during the day, and high ratios would be expected. Based on the isoprene oxidation mechanism discussed by *Carter and Atkinson* [1996], and following the expression described by *Stroud et al.* [2001] for the time rate of change in MAC/isoprene and MVK/isoprene ratios as a function of [OH], the rate coefficients, and the time available for processing, it is possible to quantify the expected ratios and to compare them with actual data. Figure 9 shows the scatterplot of MVK/isoprene versus MAC/isoprene during the daytime hours (09:00–16:00 LST) for all data. Here, the average measured daytime OH mixing ratio was assumed to be 8×10^6 molecules cm^{-3}, obtained in a rural area, about 60 km NW of Guangzhou in the PRD [*Hofzumahaus et al.*, 2009]. It is noteworthy that this methodology assumes that no fresh emissions of the parent compound i.e. isoprene are introduced or isoprene emissions are constant during the process, and the expression is purely chemical and does not include any mixing processes which might influence the observed ratio during transport. It can be seen that the measured data fit the predicted line well, though more of the measured data were above the predicted line, consistent with the observations of *Stroud et al.* [2001] and *Apel et al.* [2002]. This might be caused by a continuous (i.e. anthropogenic sources identified in section 3.1.3) MVK source which superimposed onto the daytime levels of isoprene photochemical products. Assuming that the wind speed was 2.5 m s^{-1} at the site (Guo et al., submitted manuscript, 2012), and the average distance between the center of the emitting trees and the sampling site was 5 km, the air parcel from upwind locations i.e. the mountain foot at a local scale and/or inland PRD at a regional scale would spend about 0.56–1.6 hours to arrive at the sampling site. This is enough time to significantly impact the daytime ratio because the lifetimes of MAC and MVK by OH loss are 1.0 and 1.9 hours, respectively, assuming daytime OH = 8×10^6 molecules cm^{-3}. Isoprene transport time, i.e. the time between emission and measurement of isoprene, were estimated by comparing the measured ratios with the derived trend line. The isoprene transport time was between 10 and 64 min with an average value around 30 min. The result in this study is consistent with that (~40 min) of *Stroud et al.* [2001] in which the sampling site was ~200 m away from large forests, and different from the finding (~6 min) of *Apel et al.* [2002] in

which the air was sampled above a strongly-emitting canopy. The differences in isoprene transport time among the studies were mainly caused by the OH mixing ratio which can vary spatially and temporarily, and by the proximity to the isoprene source. For instance, the average isoprene transport time will be significantly increased to 80 min when the daytime OH level is 3×10^6 molecules cm^{-3}. In contrast, it will be decreased to about 15 min while the OH concentration is 16×10^6 molecules cm^{-3}. In this study, the sampling site was about 5 km away from the center of the large forests and 15 km distance from the nearest city in inland PRD. Also, mixing was not taken into consideration when the predicted line was estimated. It is noteworthy that due to the short transport time, isoprene in the regionally transported air should be completely consumed before arriving at the sampling site, and the isoprene mixing ratio was dominated by nearby "non-local" emissions.

3.3. Contribution of Isoprene to Ozone Production

[30] It is well known that isoprene oxidation will eventually contribute to the ozone production in the atmosphere. Based on the isoprene oxidation mechanism, *Biesenthal et al.* [1997] found that if the number 5.0 is divided by the slope of a regression of total O_3 versus MVK mixing ratio, the fraction of the total O_3 production resulting from isoprene oxidation by OH can be obtained. It is assumed that MVK is rapidly produced. It is also noteworthy that this estimation is only valid under conditions where the isoprene oxidation rate is much faster than the MVK oxidation rate [*Biesenthal et al.*, 1997], which is the case for this study as the estimated isoprene photochemical age (transport time) was 30 min and the MVK lifetime was 1.9 hours. In this study, we treated the total mixing ratio of $O_3 + NO_2$ as total O_3, and we used the slope of $[O_3 + NO_2]$ versus [MVK] for daytime data of 40.1 ppbv $ppbv^{-1}$ (data not shown here). Hence, 5.0/40.1 equals 0.125, i.e. 12.5% of the ozone production resulted from OH reaction with isoprene. This is in accord with the simulation results (10–11%) of an observation-based model using the same dataset. The detailed discussion of the modeling results was given in Z. H. Ling et al. (Contribution of biogenic volatile organic compounds to photochemical ozone formation: Application of an observation based model, manuscript in preparation, 2012). It is noteworthy that any destruction of MVK by OH radicals would increase the slope of the $[O_3 + NO_2]$ – MVK regression, and subsequently decreased the calculated fraction contribution to ozone production by isoprene. Furthermore, this estimation did not consider the additional contribution to ozone formation by isoprene's oxidation products i.e. MVK and MAC.

4. Summary and Conclusions

[31] In this study, isoprene and its photochemical products MAC and MVK were monitored on 20 selected days during a 3-month comprehensive field measurement campaign at a mountain site in Hong Kong. In total, 201 hourly samples were collected. The isoprene mixing ratios were lower than most previous studies, most likely due to the fact that lower temperature played a more important role in reducing isoprene emissions at this subtropical mountain summit site. The average isoprene level on non-ozone episode days was two times that on ozone episode days ($p < 0.01$), whereas MVK showed the opposite trend, reflecting the fact that isoprene emissions were lower and transport of MVK from anthropogenic sources to the mountain site increased MVK levels on O_3 episode days. The higher daytime MVK/MAC ratio was mainly caused by the different reactivity of MVK and MAC with oxidant radicals and secondarily by anthropogenic MVK sources, whereas the greater nighttime MVK/MAC ratio was attributed to NO_3 chemistry and regional transport of anthropogenic MVK sources. Additionally, the nighttime MVK and MAC levels remained high, implying that anthropogenic sources such as vehicular emissions and industrial emissions in inland PRD region might be responsible.

[32] Analysis of the ratios of MVK and MAC to isoprene indicated that the photochemical age of measured isoprene (i.e. 10–64 min) was consistent with the photochemical lifetime of isoprene ($t = 20$ min at $[OH] = 8 \times 10^6$ molecules cm^{-3}). Thus, most air masses containing isoprene that reached the sampling point had sufficient time to completely react with OH, yielding higher ratios of MVK and MAC to isoprene. Further investigation on the relationship between MAC and MVK found that isoprene oxidation dominated the daytime MVK to MAC ratio whereas the regional transport of anthropogenic sources determined the nighttime MVK/MAC ratios.

[33] Based on the isoprene oxidation mechanism, using the slope of $[O_3 + NO_2]$ versus [MVK] for daytime data, we found that about 12.5% of the ozone production in this study resulted from OH reaction with isoprene. This was confirmed by the model simulation of an observation-based model, which estimated that 10–11% of the ozone production was due to the OH reaction with isoprene.

[34] Overall, isoprene oxidation in this subtropical ecosystem is consistent with our basic understanding of that from other ecosystems, but there is a clear additional contribution to MVK and MAC levels at this site caused by air masses enriched in MVK and MAC arriving from upwind continental regions.

[35] **Acknowledgments.** We thank the Research Grant Committee of the Hong Kong Special Administrative Region for their support via grants PolyU5179/09E and N_PolyU545/09. We are grateful to Yu Yufan, Choi Yu-Leung, Chan Wai-Lun, Tam Wai Fan and Shen Yi for their technical support. The comments from anonymous reviewers are highly appreciated. This study is partly supported by the internal grant of the Hong Kong Polytechnic University (A-PK25).

References

Apel, E. C., J. G. Calvert, T. M. Gilpin, F. C. Fehsenfeld, D. D. Parrish, and W. A. Lonneman (1999), The nonmethane hydrocarbon intercomparison experiment (NOMHICE): Task 3, *J. Geophys. Res.*, *104*(D21), 26,069–26,086, doi:10.1029/1999JD900793.

Apel, E. C., et al. (2002), Measurement and interpretation of isoprene fluxes and isoprene, methacrolein, and methyl vinyl ketone mixing ratios at the PROPHET site during the 1998 Intensive, *J. Geophys. Res.*, *107*(D3), 4034, doi:10.1029/2000JD000225.

Apel, E. C., J. G. Calvert, T. M. Gilpin, F. Fehsenfeld, and W. A. Lonneman (2003), Nonmethane hydrocarbon intercomparison experiment (NOMHICE): Task 4, ambient air, *J. Geophys. Res.*, *108*(D9), 4300, doi:10.1029/2002JD002936.

Atkinson, R. (1997), Gas phase tropospheric chemistry of volatile organic compounds: 1. Alkanes and alkenes, *J. Phys. Chem. Ref. Data*, *26*, 215–290, doi:10.1063/1.556012.

Atkinson, R. (2000), Atmospheric chemistry of VOCs and NO_x, *Atmos. Environ.*, *34*, 2063–2101, doi:10.1016/S1352-2310(99)00460-4.

Baker, B., M. Graessli, A. Guenther, N. Li, A. Huang, and J. H. Bai (2005), Biogenic volatile organic compound emission rates from urban vegetation in southeast China, *Eos Trans. AGU*, *86*(52), Fall Meet. Suppl., Abstract A51B-0057.

Biesenthal, T. A., and P. B. Shepson (1997), Observations of anthropogenic inputs of the isoprene oxidation products methyl vinyl ketone and methacrolein to the atmosphere, *Geophys. Res. Lett.*, *24*, 1375–1378, doi:10.1029/97GL01337.

Biesenthal, T. A., Q. Wu, P. B. Shepson, H. A. Wiebe, K. G. Anlauf, and G. I. Mackay (1997), A study of relationships between isoprene, its oxidation products, and ozone, in the Lower Fraser Valley, BC, *Atmos. Environ.*, *31*, 2049–2058, doi:10.1016/S1352-2310(96)00318-4.

Carter, W. P. L. (1996), Condensed atmospheric photooxidation mechanisms for isoprene, *Atmos. Environ.*, *30*, 4275–4290, doi:10.1016/1352-2310(96)00088-X.

Carter, W. P. L., and R. Atkinson (1996), Development and evaluation of a detailed mechanism for the atmospheric reactions of isoprene and NO_x, *Int. J. Chem. Kinet.*, *28*, 497–530, doi:10.1002/(SICI)1097-4601(1996)28:7<497::AID-KIN4>3.0.CO;2-Q.

Chen, H., et al. (2010), Biogenic volatile organic compounds (BVOC) in ambient air over Hong Kong: Analytical methodology and field measurement, *Int. J. Environ. Anal. Chem.*, *90*(13), 988–999, doi:10.1080/03067310903108360.

Cleveland, C. C., and J. B. Yavitt (1997), Consumption of atmospheric isoprene in soil, *Geophys. Res. Lett.*, *24*, 2379–2382, doi:10.1029/97GL02451.

Colman, J. J., A. L. Swanson, S. Meinardi, B. C. Sive, D. R. Blake, and F. S. Rowland (2001), Description of the analysis of a wide range of volatile organic compounds in whole air samples collected during PEM-Tropics A and B, *Anal. Chem.*, *73*, 3723–3731, doi:10.1021/ac010027g.

Crutzen, P. J. (1995), Ozone in the troposphere, in *Composition, Chemistry and Climate of the Atmosphere*, edited by H. B. Singh, pp. 349–393, Van Nostrand Reinhold, New York.

Dreyfus, G. B., G. W. Schade, and A. H. Goldstein (2002), Observational constraints on the contribution of isoprene oxidation to ozone production on the western slope of the Sierra Nevada, California, *J. Geophys. Res.*, *107*(D19), 4365, doi:10.1029/2001JD001490.

Fan, J., and R. Zhang (2004), Atmospheric oxidation mechanism of isoprene, *Environ. Chem.*, *1*, 140–149, doi:10.1071/EN04045.

Geyer, A., R. Ackermann, R. Dubois, B. Lohrmann, T. Muller, and U. Platt (2001), Long term observation of nitrate radicals in the continental layer near Berlin, *Atmos. Environ.*, *35*, 3619–3631, doi:10.1016/S1352-2310(00)00549-5.

Guenther, A. (2008), Are plant emissions green?, *Nature*, *452*, 701–702, doi:10.1038/452701a.

Guenther, A., et al. (1995), A global model of natural volatile organic compound emissions, *J. Geophys. Res.*, *100*, 8873–8892, doi:10.1029/94JD02950.

Guo, H., et al. (2009), Concurrent observations of air pollutants at two sites in the Pearl River Delta and the implication of regional transport, *Atmos. Chem. Phys.*, *9*, 7343–7360, doi:10.5194/acp-9-7343-2009.

Hakola, H., V. Tarvainen, T. Laurila, V. Hiltunen, H. Hellen, and P. Keronen (2003), Seasonal variation of VOC concentrations above a boreal coniferous forest, *Atmos. Environ.*, *37*, 1623–1634, doi:10.1016/S1352-2310(03)00014-1.

Hofzumahaus, A., et al. (2009), Amplified trace gas removal in the troposphere, *Science*, *324*, 1702–1704, doi:10.1126/science.1164566.

Hurst, J. M., et al. (2001), Investigation of the nighttime decay of isoprene, *J. Geophys. Res.*, *106*, 24,335–24,346, doi:10.1029/2000JD900727.

Iannone, R., R. Koppmann, and J. Rudolph (2009), $^{12}C/^{13}C$ kinetic isotope effects of the gas-phase reactions of isoprene, methacrolein, and methyl vinyl ketone with OH radicals, *Atmos. Environ.*, *43*, 3103–3110, doi:10.1016/j.atmosenv.2009.03.006.

Ingham, T., R. W. Walker, and R. E. Woolford (1994), Kinetic parameters for the initiation reaction $RH + O_2 \rightarrow R + HO_2$, paper presented at 25th Symposium (International) on Combust., Combust. Inst., Pittsburgh, Pa.

Intergovernmental Panel on Climate Change (1992), *Scientific Assessment of Climate Change*, edited by J. T. Houghton, G. J. Jenkins, and J. J. Ephraums, Cambridge Univ. Press, Cambridge, U. K.

Jiang, F., H. Guo, T. J. Wang, H. R. Cheng, X. M. Wang, I. J. Simpson, A. J. Ding, S. M. Saunders, S. H. M. Lam, and D. R. Blake (2010), An ozone episode in the Pearl River Delta: Field observation and model simulation, *J. Geophys. Res.*, *115*, D22305, doi:10.1029/2009JD013583.

Jones, C. E., J. R. Hopkins, and A. C. Lewis (2011), In situ measurements of isoprene and monoterpenes within a south-east Asian tropical rainforest, *Atmos. Chem. Phys.*, *11*, 6971–6984, doi:10.5194/acp-11-6971-2011.

Karl, T., A. Guenther, R. J. Yokelson, J. Greenberg, M. Potosnak, D. R. Blake, and P. Artaxo (2007), The tropical forest and fire emissions experiment: Emission, chemistry, and transport of biogenic volatile organic compounds in the lower atmosphere over Amazonia, *J. Geophys. Res.*, *112*, D18302, doi:10.1029/2007JD008539.

Karl, T., A. Guenther, A. Turnipseed, G. Tyndall, P. Artaxo, and S. Martin (2009), Rapid formation of isoprene photo-oxidation products observed in Amazonia, *Atmos. Chem. Phys.*, *9*, 7753–7767, doi:10.5194/acp-9-7753-2009.

Karl, T., et al. (2010), Efficient atmospheric cleansing of oxidized organic trace gases by vegetation, *Science*, *330*, 816–819, doi:10.1126/science.1192534.

Kim, S., A. Guenther, T. Karl, and J. Greenberg (2011), Contributions of primary and secondary biogenic VOC to total OH reactivity during the CABINEX (Community Atmosphere-Biosphere INteractions EXperiments)-09 field campaign, *Atmos. Chem. Phys.*, *11*, 8613–8623, doi:10.5194/acp-11-8613-2011.

Kuhn, U., S. Rottenberger, T. Biesenthal, A. Wolf, G. Schebeske, P. Ciccioli, E. Brancaleoni, M. Frattoni, T. M. Tavares, and J. Kesselmeier (2002), Isoprene and monoterpene emissions of Amazonian tree species during the wet season: Direct and indirect investigations on controlling environmental functions, *J. Geophys. Res.*, *107*(D20), 8071, doi:10.1029/2001JD000978.

Kuhn, U., et al. (2007), Isoprene and monoterpene fluxes from Central Amazonian rainforest inferred from tower-based and airborne measurements, and implications on the atmospheric chemistry and the local carbon budget, *Atmos. Chem. Phys.*, *7*, 2855–2879, doi:10.5194/acp-7-2855-2007.

Kwok, E. S. C., S. M. Aschmann, J. Arey, and R. Atkinson (1996), Product formation from the reaction of the NO_3 radical with isoprene and rate constants for the reactions of methacrolein and methyl vinyl ketone with the NO_3 radical, *Int. J. Chem. Kinet.*, *28*, 925–934.

Lacis, A. A., D. J. Wuebbles, and J. A. Logan (1990), Radiative forcing of climate by changes in the vertical distribution of ozone, *J. Geophys. Res.*, *95*, 9971–9981, doi:10.1029/JD095iD07p09971.

Leung, D. Y. C., P. Wong, B. K. H. Cheung, and A. Guenther (2010), Improved land cover and emission factor for modeling biogenic volatile organic compounds emissions from Hong Kong, *Atmos. Environ.*, *44*, 1456–1468, doi:10.1016/j.atmosenv.2010.01.012.

Montzka, S. A., M. Trainer, P. D. Goldan, W. C. Kuster, and F. C. Fehsenfeld (1993), Isoprene and its oxidation products, methyl vinyl ketone and methacrolein, in the rural troposphere, *J. Geophys. Res.*, *98*, 1101–1111, doi:10.1029/92JD02382.

Myoshi, A., S. Hatakeyama, and N. Washida (1994), OH radical-initiated photo-oxidation of isoprene: An estimate of global CO production, *J. Geophys. Res.*, *99*, 18,787–18,799.

Navarro, M. A., S. Dusanter, R. A. Hites, and P. S. Stevens (2011), Radical dependence of the yields of methacrolein and methyl vinyl ketone from the OH-initiated oxidation of isoprene under NO_x-free conditions, *Environ. Sci. Technol.*, *45*, 923–929, doi:10.1021/es103147w.

New Jersey Department of Health and Senior Services (NJDHSS) (2000), Methyl vinyl ketone: Hazardous substance fact sheet, Trenton, N. J.

New Jersey Department of Health and Senior Services (NJDHSS) (2001), Methacrolein: Hazardous substance fact sheet, Trenton, N. J.

National Research Council (1991), *Rethinking the Ozone Problem in Urban and Regional Air Pollution*, 500 pp., Natl. Acad. of Sci. Press, Washington, D. C.

Olivier, J. G. J., et al. (1996), Description of EDGAR Version 2.0: A set of global emission inventories of greenhouse gases and ozone-depleting substances for all anthropogenic and most natural sources on a per country basis and on $1^\circ \times 1^\circ$ grid, *Rep. 771060-002/TNO-MEP R96/119*, Natl. Inst. of Public Health and the Environ., Bilthoven, Netherlands.

Park, C., G. W. Schade, and I. Boedeker (2011), Characteristic of the flux of isoprene and its oxidation products in an urban area, *J. Geophys. Res.*, *116*, D21303, doi:10.1029/2011JD015856.

Roberts, J. M., et al. (2006), Analysis of the isoprene chemistry observed during the New England Air Quality Study (NEAQS) 2002 intensive experiment, *J. Geophys. Res.*, *111*, D23S12, doi:10.1029/2006JD007570.

Saunders, S. M., M. E. Jenkin, R. G. Derwent, and M. J. Pilling (2003), Protocol for the development of the Master Chemical Mechanism, MCM v3 (Part A): Tropospheric degradation of non-aromatic volatile organic compounds, *Atmos. Chem. Phys.*, *3*, 161–180, doi:10.5194/acp-3-161-2003.

Sillman, S., et al. (2002), Loss of isoprene and sources of nighttime OH radicals at a rural site in the U.S.: Results from photochemical models, *J. Geophys. Res.*, *107*(D5), 4043, doi:10.1029/2001JD000449.

Simpson, I. J., et al. (2010), Characterization of trace gases measured over Alberta oil sands mining operations: 76 speciated C_2-C_{10} volatile organic compounds (VOCs), CO_2, CH_4, CO, NO, NO_2, NO_y, O_3 and SO_2, *Atmos. Chem. Phys.*, *10*, 11,931–11,954, doi:10.5194/acp-10-11931-2010.

Simpson, I. J., et al. (2011), Boreal forest fire emissions in fresh Canadian smoke plumes: C_1-C_{10} volatile organic compounds (VOCs), CO_2, CO,

NO_2, NO, HCN and CH_3CN, *Atmos. Chem. Phys.*, *11*, 6445–6463, doi:10.5194/acp-11-6445-2011.

So, K. L., and T. Wang (2004), C-3-C-12 non-methane hydrocarbons in subtropical Hong Kong: Spatial-temporal variations, source-receptor relationships and photochemical reactivity, *Sci. Total Environ.*, *328*(1-3), 161–174, doi:10.1016/j.scitotenv.2004.01.029.

Spaulding, R. S., G. W. Schade, A. H. Goldstein, and M. J. Charles (2003), Characterization of secondary atmospheric photooxidation products: Evidence for biogenic and anthropogenic sources, *J. Geophys. Res.*, *108*(D8), 4247, doi:10.1029/2002JD002478.

Starn, T. K., P. B. Shepson, D. D. Riemer, R. G. Zika, and K. Olzyna (1998a), Nighttime isoprene chemistry at an urban-impacted forest site, *J. Geophys. Res.*, *103*, 22,437–22,447, doi:10.1029/98JD01201.

Starn, T. K., P. B. Shepson, S. B. Bertman, J. S. White, B. G. Splawn, D. D. Riemer, R. G. Zika, and K. Olszyna (1998b), Observations of isoprene chemistry and its role in ozone production at a semirural site during the 1995 Southern Oxidants Study, *J. Geophys. Res.*, *103*(D17), 22,425–22,435, doi:10.1029/98JD01279.

Stroud, C. A., et al. (2001), Isoprene and its oxidation products, methacrolein and methylvinyl ketone, at an urban forested site during the 1999 Southern Oxidants Study, *J. Geophys. Res.*, *106*(D8), 8035–8046, doi:10.1029/2000JD900628.

Stroud, C. A., et al. (2002), Nighttime isoprene trends at an urban forested site during the 1999 Southern Oxidant Study, *J. Geophys. Res.*, *107*(D16), 4291, doi:10.1029/2001JD000959.

Tang, J. H., et al. (2007), Characteristics and diurnal variations of NMHCs at urban, suburban, and rural sites in the Pearl River Delta and a remote site in South China, *Atmos. Environ.*, *41*(38), 8620–8632, doi:10.1016/j.atmosenv.2007.07.029.

Vrekoussis, M., M. Kanakidou, N. Mihalopoulos, P. J. Crutzen, J. Lelieveld, D. Perner, H. Berresheim, and E. Baboukas (2004), Role of the NO_3 radicals in the oxidation processes in the eastern Mediterranean troposphere during the MINOS campaign, *Atmos. Chem. Phys.*, *4*, 169–182, doi:10.5194/acp-4-169-2004.

Vrekoussis, M., N. Mihalopoulos, E. Gerasopoulos, M. Kanakidou, P. J. Crutzen, and J. Lelieveld (2007), Two-year of NO_3 radical observations in the boundary layer over the Eastern Mediterranean, *Atmos. Chem. Phys.*, *7*, 315–327, doi:10.5194/acp-7-315-2007.

Wang, T., H. Guo, D. R. Blake, Y. H. Kwok, I. J. Simpson, and Y. S. Li (2005), Measurements of trace gases in the inflow of South China Sea background air and outflow of regional pollution at Tai O, southern China, *J. Atmos. Chem.*, *52*, 295–317, doi:10.1007/s10874-005-2219-x.

Warneck, P. (2000), Hydrogens, halocarbons, and other volatile organic compounds, in *Chemistry of the Natural Atmosphere*, pp. 264–345, Academic, San Diego, Calif.

Yokouchi, Y. (1994), Seasonal and diurnal variation of isoprene and its reaction products in a semi-rural area, *Atmos. Environ.*, *28*, 2651–2658, doi:10.1016/1352-2310(94)90438-3.

Zhang, Y. H., K. S. Shao, X. Y. Tang, and J. L. Li (1998), The study of urban photochemical smog pollution in China, *Acta Sci. Nat. Univ. Pekinensis*, *34*, 393–399.